Carbon Dioxide Capture for Storage in Deep Geologic Formations – Results from the CO_2 Capture Project

Capture and Separation of Carbon Dioxide from Combustion Sources

Edited by

David C. Thomas
Senior Technical Advisor
Advanced Resources International, Inc.
4603 Clearwater Lane
Naperville, IL, USA

Volume 1

ELSEVIER
2005

Amsterdam – Boston – Heidelberg – London – New York – Oxford
Paris – San Diego – San Francisco – Singapore – Sydney – Tokyo

Elsevier Internet Homepage – http://www.elsevier.com
Consult the Elsevier homepage for full catalogue information on all books, major reference works, journals, electronic products and services.

Elsevier Titles of Related Interest

AN END TO GLOBAL WARMING
L.O. Williams
ISBN: 0-08-044045-2, 2002

FUNDAMENTALS AND TECHNOLOGY OF COMBUSTION
F. El-Mahallawy, S. El-Din Habik
ISBN: 0-08-044106-8, 2002

GREENHOUSE GAS CONTROL TECHNOLOGIES: 6TH INTERNATIONAL CONFERENCE
John Gale, Yoichi Kaya
ISBN: 0-08-044276-5, 2003

MITIGATING CLIMATE CHANGE: FLEXIBILITY MECHANISMS
T. Jackson
ISBN: 0-08-044092-4, 2001

Related Journals:
Elsevier publishes a wide-ranging portfolio of high quality research journals, encompassing the energy policy, environmental, and renewable energy fields. A sample journal issue is available online by visiting the Elsevier web site (details at the top of this page). Leading titles include:

Energy Policy
Renewable Energy
Energy Conversion and Management
Biomass & Bioenergy
Environmental Science & Policy
Global and Planetary Change
Atmospheric Environment
Chemosphere – Global Change Science
Fuel, Combustion & Flame
Fuel Processing Technology

All journals are available online via ScienceDirect: www.sciencedirect.com

To Contact the Publisher
Elsevier welcomes enquiries concerning publishing proposals: books, journal special issues, conference proceedings, etc. All formats and media can be considered. Should you have a publishing proposal you wish to discuss, please contact, without obligation, the publisher responsible for Elsevier's Energy program:

Henri van Dorssen
Publisher
Elsevier Ltd
The Boulevard, Langford Lane
Kidlington, Oxford
OX5 1GB, UK

Phone: +44 1865 84 3682
Fax: +44 1865 84 3931
E.mail: h.dorssen@elsevier.com

General enquiries, including placing orders, should be directed to Elsevier's Regional Sales Offices – please access the Elsevier homepage for full contact details (homepage details at the top of this page).

ELSEVIER B.V.
Radarweg 29
P.O. Box 211, 1000 AE Amsterdam
The Netherlands

ELSEVIER Inc.
525 B Street, Suite 1900
San Diego, CA 92101-4495
USA

ELSEVIER Ltd
The Boulevard, Langford Lane
Kidlington, Oxford OX5 1GB
UK

ELSEVIER Ltd
84 Theobalds Road
London WC1X 8RR
UK

First edition 2005

Library of Congress Cataloging in Publication Data
A catalog record is available from the Library of Congress.

British Library Cataloguing in Publication Data
A catalogue record is available from the British Library.

ISBN: 0-08-044570-5 (2 volume set)

Volume 1: Chapters 8, 9, 13, 14, 16, 17, 18, 24 and 32 were written with support of the U.S. Department of Energy under Contract No. DE-FC26-01NT41145. The Government reserves for itself and others acting on its behalf a royalty-free, non-exclusive, irrevocable, worldwide license for Governmental purposes to publish, distribute, translate, duplicate, exhibit and perform these copyrighted papers. EU co-funded work appears in chapters 19, 20, 21, 22, 23, 33, 34, 35, 36 and 37. Norwegian Research Council (Klimatek) co-funded work appears in chapters 1, 5, 7, 10, 12, 15 and 32.

Volume 2: The Storage Preface, Storage Integrity Preface, Monitoring and Verification Preface, Risk Assessment Preface and Chapters 1, 4, 6, 8, 13, 17, 18, 19, 20, 21, 22, 23, 24, 25, 26, 27, 28, 29, 30, 31, 32, 33 were written with support of the U.S. Department of Energy under Contract No. DE-FC26-01NT41145. The Government reserves for itself and others acting on its behalf a royalty-free, non-exclusive, irrevocable, worldwide license for Governmental purposes to publish, distribute, translate, duplicate, exhibit and perform these copyrighted papers. Norwegian Research Council (Klimatek) co-funded work appears in chapters 9, 15 and 16.

♾ The paper used in this publication meets the requirements of ANSI/NISO Z39.48-1992 (Permanence of Paper).
Printed in The Netherlands.

Carbon Dioxide Capture for Storage in Deep Geologic Formations, Volume 1
D.C. Thomas and S.M. Benson (Eds.)

Chapter 13

DEVELOPMENT OF THE SORPTION ENHANCED WATER GAS SHIFT PROCESS

Rodney J. Allam[1], Robert Chiang[2], Jeffrey R. Hufton[2], Peter Middleton[3], Edward L. Weist[2] and Vince White[1]

[1]Air Products PLC, Walton-on-Thames, UK
[2]Air Products and Chemicals, Inc., Allentown, PA, USA
[3]BP plc, Sunbury-on-Thames, UK

ABSTRACT

The CO_2 Capture Project (CCP), working with Air Products and Chemicals and with funding support of the US DOE, has undertaken development of a novel precombustion decarbonization technology referred to as the sorption enhanced water gas shift (SEWGS) process. This technology is particularly attractive for decarbonizing gas turbine fuel, and hence provides opportunities for power generation with minimal CO_2 emissions, high power efficiency and potentially lower cost of capturing CO_2 for storage.

The SEWGS process simultaneously converts syngas containing CO into H_2 and CO_2 and removes the CO_2 from the product hydrogen by adsorption. The system operates as a multi-bed pressure swing adsorption unit, with each bed packed with a mixture of shift catalyst and a high-temperature CO_2 adsorbent. Carbon in the feed gas in the form of CO and CO_2 are removed from the product gas by the CO_2 adsorbent, and after specific PSA process steps, rejected as relatively high-purity CO_2 for recovery. The product hydrogen produced during the feed step contains the excess steam from the reaction and any nitrogen from the syngas generation, and is at high temperature and feed pressure. This hot fuel mixture can be burned in gas turbines with higher turbine efficiency than with natural gas firing and substantially lower NO_x formation.

During a 2-year development program, the key process performance and design issues were studied through a combination of experimental work, simulation and techno-economic evaluation. The experimental program developed and characterized candidate adsorbents in a range of tests including thermogravimetric analysis and the use of a cyclic process test unit. Many potential CO_2 adsorbent materials were screened prior to identification of the leading material, a promoted hydrotalcite (HTC), which showed the highest cyclic capacity for removal of CO_2 under the conditions of interest. Detailed parametric studies were conducted with this material to provide the sizing data for design of full-scale SEWGS units. Proof-of-concept test runs were conducted in the process test unit with a model syngas feed containing CO, H_2 and CO_2, which was fed in breakthrough and cyclic modes to a single bed vessel containing a mixture of catalyst and HTC. These tests demonstrated that the equilibrium limit for conventional reactors was overcome, a substantially decarbonized hydrogen product was produced, and a carbon recovery of over 80% was achieved.

Process designs were developed by APCI for two CCP case studies, a 400 MW combined cycle case and capture from multiple gas turbine drives in an oil-field gas compression system. Flow schemes were developed using autothermal reforming to produce syngas from the natural gas feed. Air blown and oxygen blown autothermal reformer schemes were prepared and overall power generation process performance was determined by ASPEN simulation. Process equipment sizing calculations and SEWGS cost estimates were

Abbreviations: CCGT, combined cycle gas turbine; HTC, hydrotalcite promoted with K_2CO_3; HTS, high temperature shift; SEWGS, sorption enhanced water gas shift process; TGA, thermal gravimetric adsorption; WGS, water gas shift.

conducted and passed, along with utility requirements, to CCP-funded cost estimators. The CCP common economic model was used to determine costs of CO_2 capture for the process in each case study and compared with the existing baseline technologies.

INTRODUCTION

This development program was supported through the precombustion subgroup of the CO_2 Capture Project (CCP). The CCP is a major joint energy industry effort to respond to concerns existing around climate change and CO_2 concentrations in the atmosphere. The CCP involves the following participant companies: BP (Co-ordination), Chevron Texaco, En Cana, Eni, Norsk Hydro, Shell, Statoil and Suncor. Program funding comes from the participating companies, along with contributions from the Department of Energy in the US, from Norway and from the European Union.

Application Scenarios

A major function of the CCP is to achieve major reductions in the cost of CO_2 capture and storage compared to existing technologies. Studies were commissioned on various technology options applied to real locations where major CO_2 emissions occur. Applicability of the sorption enhanced water gas shift (SEWGS) process in the Alaskan and Norcap scenarios was considered in this work. The former is CCP scenario (D) located at Prudhoe Bay on the Alaskan North Slope. The aim is to capture CO_2 produced by the operation of a given number and types of gas turbines. In this work, we consider the precombustion decarbonization alternative in which natural gas is converted to hydrogen, and CO_2 is separated with the SEWGS system. A total of 11 open cycle gas turbines are powered with the hydrogen fuel. Details supplied on these gas turbines are given in Table 1. The CO_2 captured in the SEWGS system is compressed 220 barg and is available for EOR applications.

TABLE 1
SUPPLIED DATA ON THE ALASKA GAS TURBINES

I.D.	Type	Model	Fuel gas flow (kg/h)	Exhaust gas flow (kg/h)	Exhaust gas temperature (°C)
1	GE Frame 6	GE MS-6001-B	12,983	548,847	480
2	GE Frame 6	GE MS-6001-B	12,983	548,847	480
3	GE Frame 6	GE MS-6001-B	12,983	548,847	480
4	GE Frame 6	GE MS-6001-B	12,983	548,847	480
5	GE Frame 5	MS-5382-C	9,621	471,737	480
6	GE Frame 5	MS-5382-C	9,621	471,737	480
7	Rolls Royce RB-211	Coberra 6456	6,889	331,123	480
8	Rolls Royce RB-211	Coberra 6456	6,889	331,123	480
9	GE Frame 5	MS-5382-C	9,621	471,737	480
10	Rolls Royce RB-211	Coberra 6456	6,889	331,123	480
11	Rolls Royce RB-211	Coberra 6456	6,889	331,123	480

The goal for the Norcap scenario is to develop a process for producing power (350 MW) with drastically reduced CO_2 emissions. In this case, a gas turbine combined cycle incorporating the General Electric 9FA turbine has been utilized. Natural gas is decarbonized and CO_2 separated with the SEWGS system. Recovered CO_2 is required at pressure (150 barg) for EOR.

Each scenario invoked a set of conditions (Table 2), which were adopted in the simulations, e.g. natural gas compositions, cooling fluid type and temperature, and degree of process modularization, among others.

Sorption Enhanced Water Gas Shift Process

The SEWGS process provides a way to simultaneously convert CO in syngas to CO_2 and remove the CO_2 from hot, hydrogen-rich product gas. It combines the water gas shift reaction with an adsorbent

TABLE 2
KEY CONDITIONS FOR THE ALASKAN AND NORCAP SCENARIOS

	Alaskan scenario	**Norcap scenario**
Natural gas composition after H_2S removal		
Methane (%)	79.80	79.77
Carbon dioxide (%)	11.92	2.92
Nitrogen (%)	0.65	0.61
Ethane (%)	5.35	9.67
C_3 (%)	1.76	4.45
C_4 (%)	0.38	1.96
C_5 (%)	0.06	0.41
C_6 (%)	0.07	0.21
Cooling medium	Glycol, 24 °C	Glycol, 19 °C or seawater, 11 °C
Modularized configuration required?	Yes	No

that simultaneously removes the product CO_2 and thus pushes the reaction further towards H_2 production. This increases the production and purity of hydrogen, increases the CO conversion, and effectively removes carbon species from the gas phase product. This high-pressure, high-temperature product gas consists of a decarbonized hydrogen/steam mixture which is used as turbine fuel. A separate CO_2 by-product can be recovered from the adsorbent by regenerating the bed. This byproduct can then be compressed and sequestered.

The advantages of combining the water gas shift reaction with separation of CO_2 are:

- Conversion of CO to H_2 in the equilibrium limited shift reaction is increased through the removal of a product of reaction—CO_2.
- Separation of CO_2 at high temperature and utilization of the hot hydrogen product minimizes heat exchange equipment.
- Hydrogen exits the reactor at high temperature with surplus process steam, which increases the overall efficiency and reduces NO_x emissions in the gas turbine.

The basic function of the SEWGS process is to drive the water gas shift reaction ($CO + H_2O \leftrightarrow CO_2 + H_2$) to the right by removing CO_2 from the reaction gas via a special high-temperature CO_2 adsorbent. The adsorbent is packed, along with shift catalyst, in multiple fixed-bed reactors. Each vessel is subjected to a sequence of process steps, i.e. the process cycle that either produces decarbonized hydrogen product gas (sorption/reaction step) or regenerates the CO_2 adsorbent. Regeneration of the adsorbent is accomplished by reducing the gas phase partial pressure of CO_2 by purging counter-currently with steam, and is hence similar to pressure swing adsorption units that are commonly used for air separation, hydrogen purification, and other gas separations.

Figure 1 illustrates the arrangement envisioned for the SEWGS process. It utilizes a 7-bed system operating in cyclic operation. The SEWGS process cycle is schematically illustrated in Figure 2. The first step is the feed, or reaction/sorption step, where raw syngas from the syngas generator (35 bar, roughly 350–450 °C) passes through the catalyst/adsorbent mixture. The CO and steam are reacted to CO_2 and H_2, and the CO_2 is removed by the adsorbent. This yields a hydrogen-rich product at essentially feed pressure and high temperature (~450–550 °C). After a specified amount of time, the feed gas is diverted to another vessel and the current vessel is regenerated.

The first step of regeneration is a CO_2 rinse step, where some of the CO_2 product is cocurrently passed through the bed. This step is necessary to obtain a relatively high-purity CO_2 product. This is not a complete

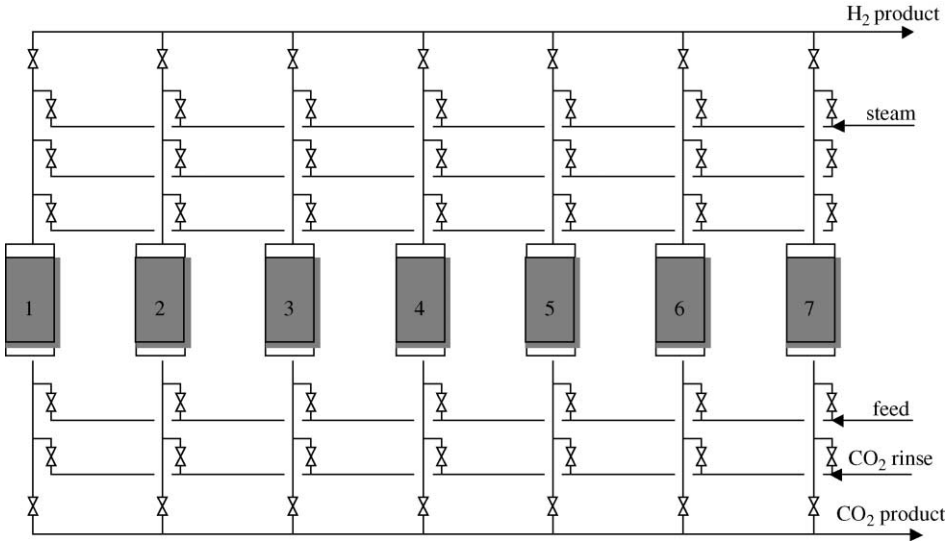

Figure 1: Schematic diagram of 7-bed cyclic sorption enhanced reactor system.

rinse; the CO_2 flow is terminated once the CO_2 front reaches one-third to one-half of the way down the bed. The effluent gas from this step is fed to another bed to recover hydrogen.

The next two steps are cocurrent pressure equalizations, in which the vessel contents are expanded into previously regenerated vessels in order to recover hydrogen and pressure energy. At the end of the last equalization step, the CO_2 front has just reached the product end of the vessel, and the gas phase is essentially CO_2.

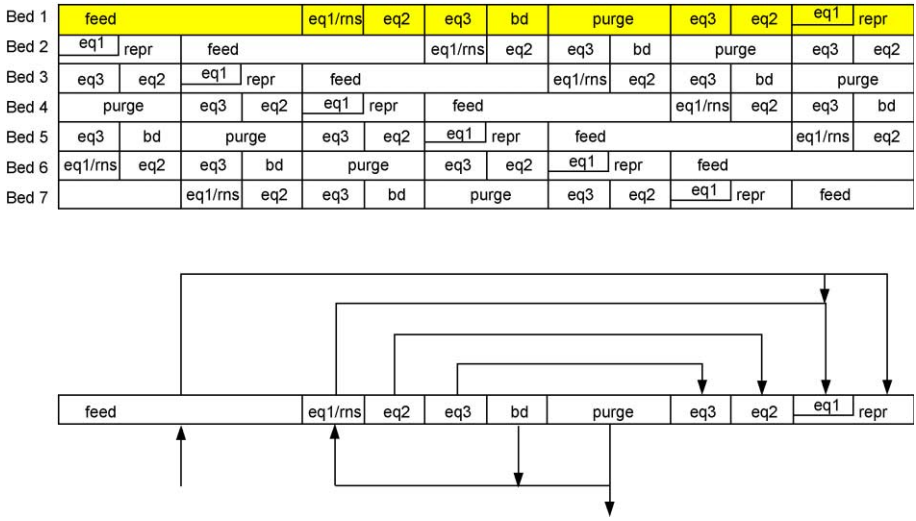

Figure 2: SEWGS process cycle (RINSE/EQ).

Recovery of CO_2 is achieved in the next two steps, blowdown and purge. The blowdown step is carried out countercurrently to a pressure of roughly 1.1 atm. Steam is then used to countercurrently purge the beds. Steam pressure must be high enough to overcome the pressure drop of the sorber/reactor and downstream piping/condenser, which typically is less than 10 psig. The effluent gas consists of 97 + $\%CO_2$ (dry basis) and steam at essentially 1 atm and 350–450 °C.

The final steps of the process are associated with repressurizing the vessels, first by accepting gas from other vessels undergoing the pressure equalization and CO_2 rinse steps, and later by receiving countercurrent product gas.

The application of the SEWGS technology in a natural gas fed CCGT scheme is indicated in Figure 3, where it is used in conjunction with an oxygen blown autothermal reformer (ATR). This flow-scheme represents integration with a large combined cycle gas turbine or multiple smaller open cycle gas turbines. In principle, the same approach can be applied to separation of CO_2 from an integrated gasification combined cycle plant using oil, coke or coal feeds.

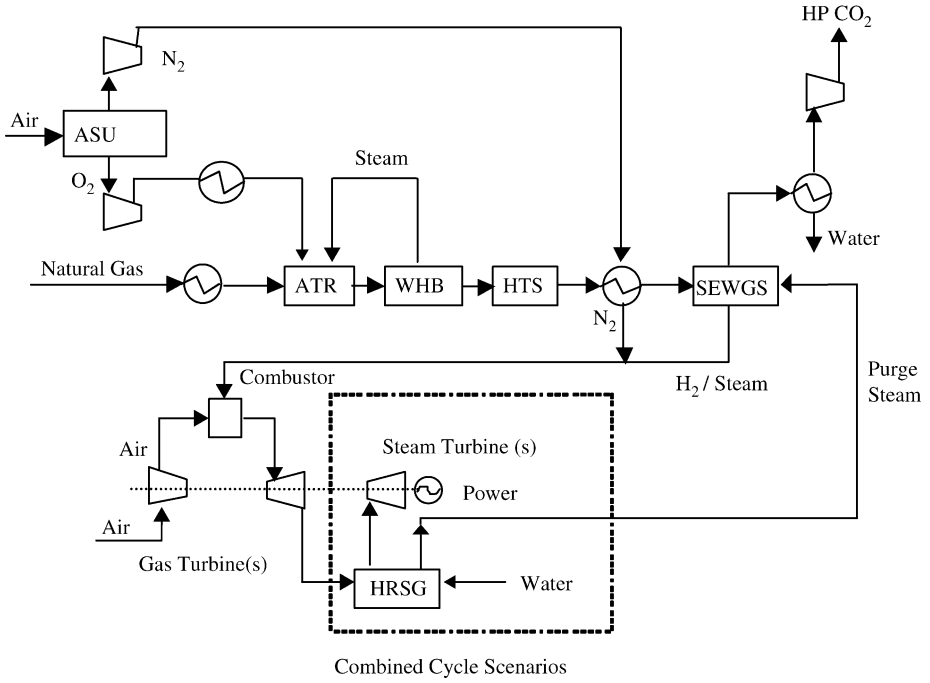

Figure 3: SEWGS system for recovery of CO_2 from gas turbine schemes.

Feed gas to the SEWGS unit is syngas, which can be produced by reaction of natural gas with oxygen and steam in an ATR via reactions (1) and (2).

$$CH_4 + \tfrac{1}{2}O_2 \leftrightarrow CO + 2H_2 \quad (1)$$

$$CH_4 + H_2O \leftrightarrow CO + 3H_2 \quad (2)$$

The ATR product is cooled in a steam-raising waste heat boiler (WHB) before undergoing shift reaction in a high temperature shift (HTS) reactor R102, where reaction (3) occurs over an iron chrome catalyst.

$$CO + H_2O \leftrightarrow CO_2 + H_2 \tag{3}$$

The equilibrium conversion of reaction (3) is favored by low temperature of reaction, but this limits the kinetic rate, hence multiple stages of reaction are used in conventional designs. To achieve high conversion, the SEWGS reactor completes the shift reaction at high temperature but in the presence of a CO_2 adsorbent.

Project Execution

A phased approach was taken during execution of this project. In phase 1, adsorption process simulations were conducted with assumed adsorbent equilibrium and kinetic parameters to estimate the SEWGS performance. These results were incorporated into steady-state simulations of the power generation process to determine the potential impact on the overall process. Economic evaluations were carried out to quantify the benefits. In phase 2, experimental efforts were directed towards the screening of high-temperature CO_2 adsorbents, characterization of the critical properties of the best materials, and demonstration of the SEWGS concept. In phase 3, a refined estimate of SEWGS process performance was developed from the experimental data, and the results were fed to the ASPEN simulations to generate detailed heat and mass balance data for both Alaskan and Norcap scenarios. Process equipment was sized, and capital and operating costs were evaluated. The results described in this chapter will generally follow this path.

EXPERIMENTAL/STUDY METHODOLOGY

Simulation Tools

Dynamic and steady-state process simulators were utilized in this study. An in-house dynamic adsorption process simulator was modified to account for reaction terms and used to model the performance of the cyclic SEWGS process. The starting algorithm has been shown to accurately predict the dynamic and cyclic steady-state behavior of many types of adsorption processes at Air Products, from relatively small, fast-cycle oxygen vacuum swing adsorption processes to state-of-the-art hydrogen pressure swing processes producing 100 MM scfd of product. Knowledge of the CO_2 adsorption properties (isotherm, mass transfer rate parameters, heat of adsorption), reaction rate constants, vessel geometry, and process cycle structure are required for these models.

Steady-state simulations of the full power generation processes were carried out with ASPEN.

Experimental Equipment

The experimental apparatuses used in this work include a modified high-temperature thermogravimetric analysis (TGA) unit and a process test unit. Detailed descriptions can be found in Ref. [1].

The TGA monitors the weight of a small sample of material (30–50 mg) exposed to flowing gas at a fixed temperature between 400–500 °C. By evaluating the change in mass, one can determine how much of the gas has been adsorbed on the sample. Our TGA was modified to permit continuous switching between carbon dioxide and nitrogen. Each gas was humidified to ~2% water via water bubblers. The exposure time per cycle between the adsorbent and each gas was between 5 min and 2 h, depending on the experiment. All gas exposure was at atmospheric pressure. The weight change measured during the 14th cycle is generally the value reported in this work.

An experimental fixed bed test unit (process test unit) was built to evaluate the performance of high-temperature CO_2 adsorbents at up to 31 barg (450 psig) and 550 °C (1025 °F). A simplified schematic of the set-up is illustrated in Figure 4. The test system consisted of a gas cylinder manifold, gas mass flow controllers, two steam generators, a single absorber vessel, air-actuated switching valves, two DTMs for flow measurement, and two IR CO_2 gas analyzers. The adsorber vessel was made of 316ss tube, 44 mm (1.75 in.) OD and 1860 mm ($73\frac{1}{4}$ in.) length from flange to flange. It was heated via an external heating blanket to a temperature between 400 and 500 °C.

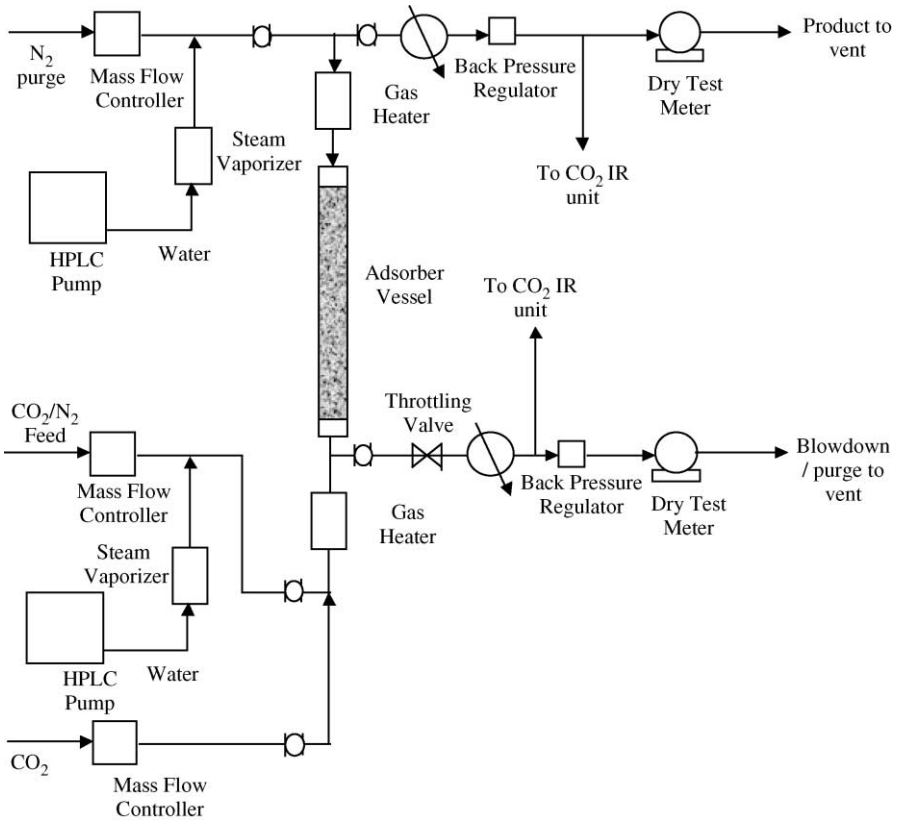

Figure 4: Schematic illustration of process test unit.

Mixtures of CO_2, N_2, and steam were used for feed gas, and N_2 and steam were used as regeneration gas. During an experiment, the adsorber was exposed to cycle steps consisting of high-pressure feed (up to 25 bar), countercurrent depressurization to 1 bar, countercurrent purge with steam/N_2 at 1 bar, and countercurrent repressurization with steam/N_2 to the feed pressure. The above steps were carried out repetitively to mimic the operation of a pressure swing adsorption unit. Process performance parameters include the purity and recovery of N_2 in the product gas, the recovery of and purity of CO_2 in the waste gas, and the effective working capacity of the adsorbent. The feed step pressure, system temperature, and flow/time for feed and purge steps was varied to determine their effect on performance.

The unit could also be operated with individual steps, e.g. by carrying out a breakthrough experiment, which is essentially a repressurization step followed by a feed step which extends until substantial CO_2 breaks through the adsorber. Desorption characteristics were also evaluated by conducting desorption experiments wherein the adsorber, saturated with feed gas, was depressurized and purged for an extended period of time. The time-dependent effluent gas purity and flow from the breakthrough and desorption experiments were analyzed to determine CO_2 adsorption capacities, mass transfer coefficients, and regeneration efficiencies.

The process test unit was later modified to permit investigation of reactive feed gases containing H_2 and CO. Infrared detectors for CH_4 and CO, in addition to CO_2, were used to measure composition of product and purge effluent gases. System operation was generally the same as described above.

Materials

Most of the adsorbents studied in this work were obtained from commercial adsorbent manufacturers (CL750, HTC, PbO, defined later). Double salt adsorbents were prepared in the lab by synthesizing them on a number of commercially available alumina supports. More details on this procedure can be found in Ref. [1]. HTS catalyst was UCI C12-4-02 (89% Fe_2O_3/8% Cr_2O_3/2% CuO) obtained from United Catalysts. Mixed feed gases (CO_2 in N_2; CO, CO_2 in H_2) and regeneration gas (N_2) were obtained from gas cylinders (Air Products). De-ionized water from Aldrich was used for steam generation.

RESULTS AND DISCUSSION

Preliminary Process Evaluations

In phase 1 of this work, various flowsheet alternatives were considered and MEA-containing flowsheets were compared against SEWGS flowsheets for the Norcap scenario. The SEWGS and MEA units were used to remove CO_2 from syngas supplied from an HTS unit, with the CO_2 product compressed for sequestration and the hydrogen-rich product used as feed for the 9FA gas turbine. For the SEWGS case, the hydrogen product gas is hot (up to around 530 °C) and contains steam, which increases the efficiency of the gas turbine relative to the MDEA system (where the hydrogen product is relatively dry and at low temperature, i.e. ~40 °C). Syngas generation was from natural gas using an ATR with either compressed air or oxygen from an air separation unit (ASU). An alternative air case was also examined that rather than use a dedicated air compressor, used compression within the gas turbine and then adiabatically boosts this pressure to the operating pressure of the ATR.

All of the flowsheet alternatives used a high-degree of heat integration in order to produce as much power as possible from steam turbines that operated with a reheat cycle at three pressure levels: 150, 35 and 4 bar. Performance of the SEWGS unit was estimated with the dynamic process simulator using assumed adsorption mass transfer rate parameters.

The results from this early phase of process simulation work are summarized in Table 3. This table shows the carbon removal efficiency and the thermal efficiency of the processes based on lower heating value of the natural gas feed. Also in this table, where calculated, are the appropriate costs for the removal of CO_2. The carbon efficiency numbers are high due to the way in which the MDEA and SEWGS systems were modeled in Aspen as perfect separators, i.e. they remove all of the CO_2 that is fed to them. Nevertheless, it is clear that the SEWGS process configuration yields a higher thermal efficiency than the MDEA-based processes, regardless of how the feed syngas is produced (air-ATR, O_2-ATR). This, along with lower capital costs, leads to a lower CO_2 removal cost for the SEWGS process configuration, even though the air-ATR efficiency is higher.

TABLE 3
SUMMARY OF INITIAL RESULTS WITH MDEA/LTS AND SEWGS

(MDEA) SEWGS	Air-ATR	Air-ATR GT Sidedraw	O^2-ATR
Carbon removal	(94.2%) 99.3%	(94.6%) 99.3%	(96.2%) 97.9%
Efficiency	(42.6%) 48.9%	(41.8%) 46.6%	(41.8%) 47.3%
Net power MW	(374) 381	(368) 365	(344) 357
$/tonne CO_2	($34.85) –	––	($30.29) $24.02

Experimental Work

Phase 1 simulation efforts indicated the SEWGS approach had potential, and the next step was to experimentally demonstrate high-temperature CO_2 adsorbents that could deliver the required performance.

Material screening

The solid-phase high-temperature CO_2 adsorbent is the heart of the SEWGS process. The material must efficiently adsorb and desorb CO_2 via pressure swing cycles (between ~30 and ~1.5 bar) at operating

temperatures of 400–550 °C. Materials studied in this work include commercial sodium oxides (CL750), K_2CO_3 promoted hydrotalcites (HTCs), lead oxide adsorbents (PbO), and double salt adsorbents (DS).

A summary of cyclic TGA data for these materials are listed in Table 4. The lead oxide materials showed limited CO_2 capacity at higher temperatures. The capacity of the CL750 sample was reasonable at 400 °C/120 min cycles, but was roughly a factor of two lower than the promoted HTC. Extensive effort was directed towards synthesis of supported double salts. Effective CO_2 adsorbents were generated, but the capacities were also inferior to the HTC material. The best material was thus found to be the K_2CO_3-promoted HTC with a TGA capacity of ~1.6 mmol/g at 400–450 °C/5 min cycle time. The results of TGA testing with different exposure times (120, 10, and 5 min) show that the CO_2 capacity is reduced by a factor of about two when the cycle is shortened from 10 to 5 min. Characterization work with this material, particularly the desorption behavior, was pursued with the process test unit.

TABLE 4
SUMMARY OF TGA DATA FOR POTENTIAL CO_2 ADSORBENTS

Material	Temperature (°C)	TGA cycle time (min)	CO_2 capacity, 14th cycle (wt%)
PbO	400	120	<0.5
CL750	400	120	1.5
DS	450	5	0.8–1.0
HTC	400	120	2.8–3.1
	400	10	2.8–3.1
	400	5	1.4–1.6

Hydrotalcite adsorption/desorption characterization

HTC is a layered double hydroxide with the chemical formula $Mg_6Al_2(OH)_{16}[CO_3]\cdot 4H_2O$. When heated, it decomposes and collapses into an active phase consisting of mixed metal oxides. An effective CO_2 adsorbent can be made by initially promoting the HTC with 20–35% K_2CO_3. Details of the structure of HTC and the promoted material can be found in previous DOE reports [2,3].

A series of breakthrough experiments was carried out with the HTC material to evaluate run-to-run stability of the CO_2 adsorption capacity. Feed gas consisted of a mixture of 15.05% CO_2 in N_2 gas mixed with steam (final feed composition 12.5% CO_2, 17.1% H_2O and balance N_2). The feed step was carried out at 355 psig, with a feed gas flow rate of either 5 or 10 slpm. After breakthrough, the adsorber vessel was depressurized to 2–10 psig and then purged countercurrently for 2.5 h with 5 lpm flow of 27% steam in N_2. The effluent CO_2 concentration was reduced to <0.3% with this treatment. Another breakthrough run was carried out after pressurizing the bed to 355 psig with 16% steam in N_2. This procedure was carried out repetitively to generate multiple breakthrough curves.

Breakthrough data were evaluated by determining the time during the feed step when the CO_2 mole fraction was half that of the feed gas, i.e. 7.5% for 15% CO_2 feed gas. This time, t_b, was then used to calculate the adsorption capacity via the following equation:

$$n_{CO2} = \frac{(t_b F - V) y_F}{M_s} \tag{4}$$

where n_{CO2} is the CO_2 adsorption capacity in mmol/g, F is the feed gas flow rate (steam and gas), V is the moles of gas in the reactor void volume at the feed step pressure, y_F is the feed gas CO_2 mole fraction (wet basis), and M_s is the total mass of adsorbent loaded into the adsorber vessel. The CO_2 mole fraction and flow rate data during the depressurization and purge steps were used to evaluate the amount of CO_2 removed during regeneration. These values were then normalized by the total amount of CO_2 initially in the column to yield the fraction of CO_2 removed (or f) and plotted versus the amount of purge gas introduced to the column. Overall and CO_2 mass balances were determined and typically found to be within 5%. The CO_2 mole fraction data for repetitive experiments were found to be very reproducible.

The CO_2 capacity evaluated over a number of cycles is illustrated in Figure 5. The capacity is around 0.8 mmol CO_2/g HTC, or 3.5 wt% (conversion is 1 mmol/g = 4.4 wt%). The capacity data show a significant decline from the first to second breakthrough of a given cycle set, which is probably due to incomplete regeneration during the cycles. There is also a slower decrease, which appears to have stabilized during the last few sets of cycles. Previous investigations with HTC during earlier programs indicated that the capacity does stabilize and is maintained even after 200 + days of cycling in a TGA [3].

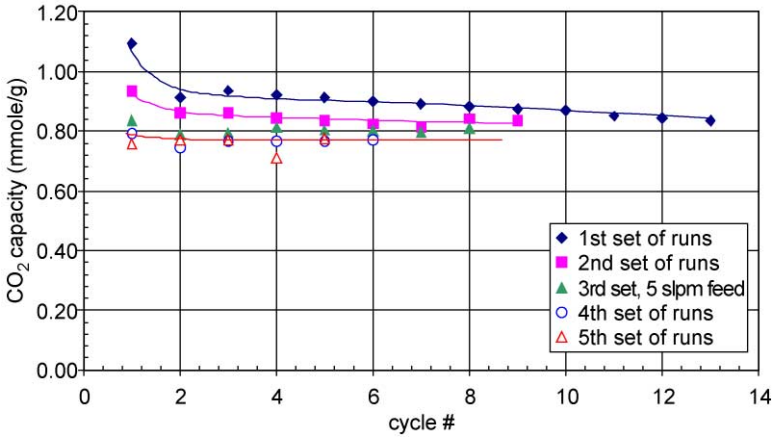

Figure 5: CO_2 adsorption capacity for repetitive cycles in fixed bed test unit; 350 psig, 12.5% CO_2, 17.1% H_2O, balance N_2, 450 °C.

CO_2 adsorption isotherm on HTC. Breakthrough data were obtained at different CO_2 partial pressures in order to define the adsorption isotherm of CO_2 on HTC. The isotherm data for 400, 450 and 500 °C are plotted in Figure 6. The trend with temperature is as expected for adsorption—higher temperature lowers the CO_2 adsorption capacity. The heat of adsorption evaluated at 0.3 and 0.6 mmol/g loading (via the Clausius–Clapeyron equation) was found to be ~10 kcal/mol. The HTC adsorbent yields a much more linear shape at

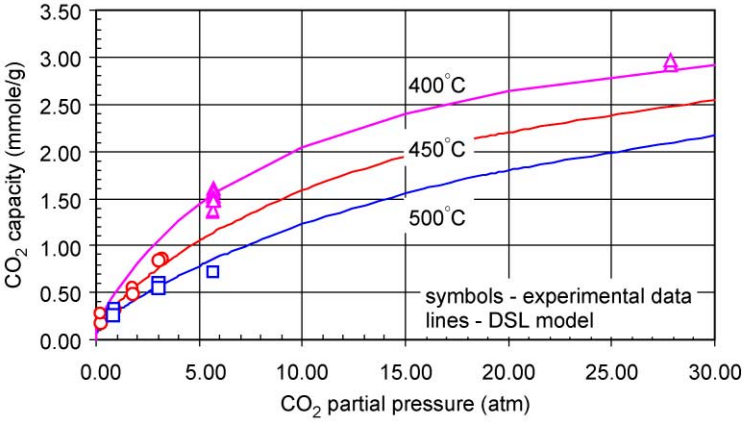

Figure 6: Adsorption isotherm for CO_2 on HTC; symbols—data, lines—model.

higher pressures than noted in previous works with other HTC samples [3]. The more linear shape is desirable, since in the absence of rate limitations, a linear isotherm is more efficiently regenerated than a steep isotherm.

Measurement of adsorption profiles at different flowrates. Breakthrough runs were carried out with feed gas containing 12.4% CO_2, 17.3% H_2O, and balance N_2 at 450 °C and 24.5 bar (355 psia). The feed gas rate was varied from 6.0 to 12.3 slpm, yielding G-rates from 2.7 to 5.5 lbmol/h/ft^2 (G-rate is the molar feed rate divided by the column cross-sectional area). The profiles are plotted in Figure 7 as the dry effluent CO_2 mole

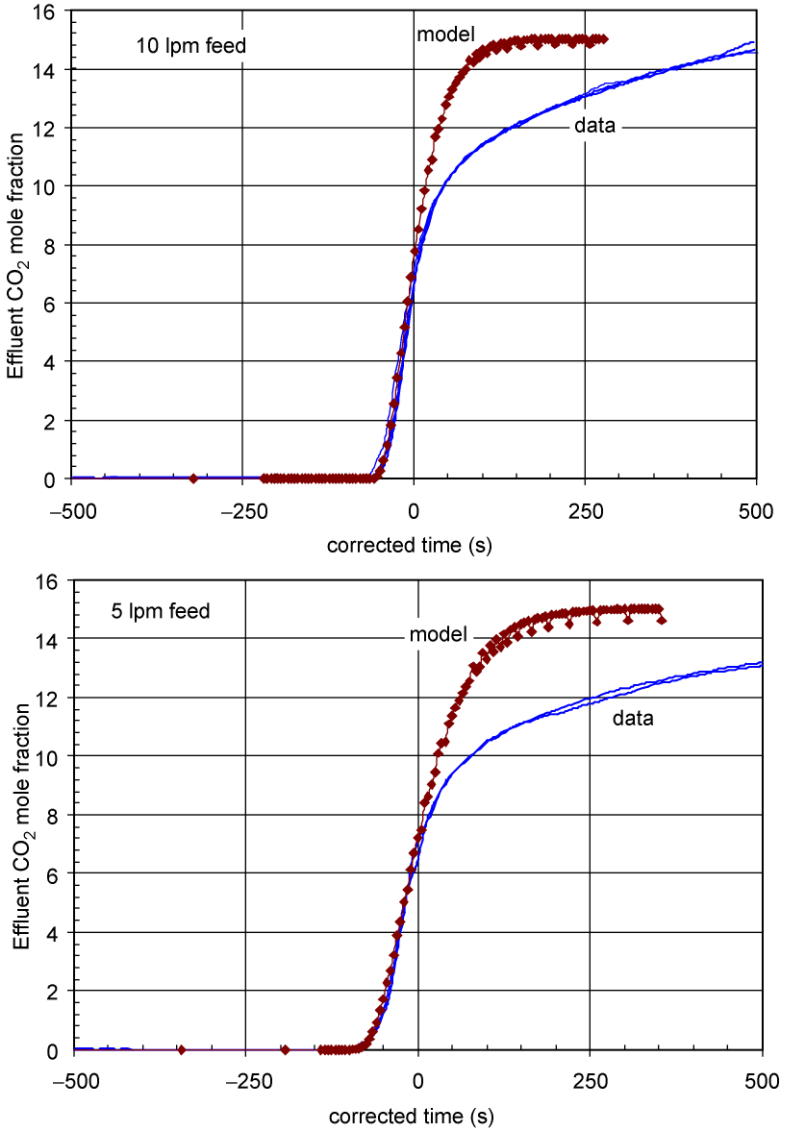

Figure 7: Comparison of experimental adsorption profile with model.

fraction versus normalized time. Reproducibility is excellent, as the data for multiple runs are essentially indistinguishable. The time scale of our process requires characterization of the leading edge of the adsorption profile, which shows a rapid increase. Breakthrough curves generated from the isothermal dynamic process simulator are also illustrated in the figure. The dual-site Langmuir isotherm was used to describe the system equilibrium, and a linear driving force model with constant mass transfer coefficients was used for mass transfer kinetics. The model with a mass transfer coefficient of 0.1 s^{-1} captures the shape of the leading edge of the profile for both feed flow rates. The value of 0.1 s^{-1} is consistent with that assumed in the Phase 1 process simulations.

It is important to point out that the highest experimental G-rate is a factor of ten lower than the Phase 1 design G-rate of 59 lbmol/h/ft^2. Adsorption kinetics could be more prevalent at the design flow rate, and further breakthrough tests should be carried out at higher feed flow rates.

Measurement of desorption profiles at different flowrates. Regeneration of the adsorbent is one of the most critical steps in an adsorption process. Ideally, the rate of CO_2 desorption is fast and limited only by adsorption equilibrium limits. In this case, a minimum amount of purge gas is needed to remove CO_2 from the column. If the rate of CO_2 desorption is relatively slow, then more purge gas will be needed to remove a similar amount of CO_2. This yields higher steam requirements for the process.

Carbon dioxide desorption experiments were carried out. Before the test, the column was saturated with 12.4% CO_2, 17.3% H_2O, and balance N_2 at 450 °C and 24.5 bar (355 psia). The column was slowly depressurized (in countercurrent direction to feed gas flow) to ~1.7 bar (~25 psia), and then a constant purge flow of 27% H_2O in N_2 was passed countercurrently for 2.5 h at ~1.7 bar and 450 °C. Purge flow rates of 3.4 and 6.9 slpm were used, yielding purge G-rates of 1.5 and 3.1 lbmol/h/ft^2 (the Phase 1 process design assumed a purge G-rate of 21 lbmol/h/ft^2). Figure 8 shows a plot of the fraction of CO_2 removed during regeneration versus the standard liters (sl) of purge gas fed to the column. On this basis, the experimental data are rather similar, with only a slight inefficiency noted for the higher purge rate run. Predictions from the dynamic simulator are included in Figure 8 for different desorption mass transfer coefficient values (k_{des}). A value of 0.1 s^{-1}, found for the adsorption rate, clearly does not describe the data. The f-curve generated with $k_{des} = 0.001$ s^{-1} describes the 6.9 lpm data relatively well, but fails to describe

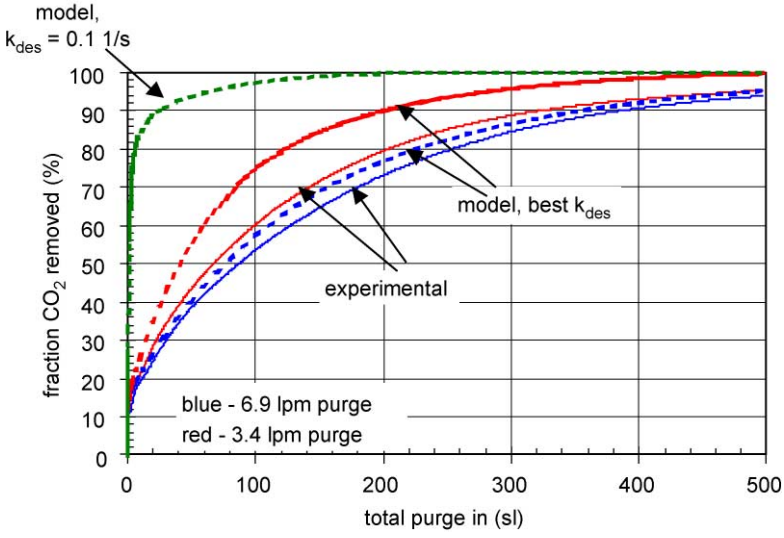

Figure 8: Comparison of experimental and model f-curves.

the 3.4 lpm data. The model predicts that doubling of the purge gas flow rate essentially doubles the amount of purge gas required for a given level of CO_2 removal. The experimental data *do not* exhibit this same level of sensitivity to the purge gas flow rate. Higher purge rates decrease the efficiency of purge, but not to the same extent that the model predicts. For this reason, we decided to base our process design calculations on the best experimental data that we could obtain rather than use the adsorption process simulator.

Regeneration with high steam content. Modifications were made to our purge steam vaporizer to permit operation at higher purge gas steam content (to 68%) and purge flow rate (to G-rate of 6.2 lbmol/h/ft^2). The column was first saturated with 20.2% CO_2, 15.8% H_2O, balance N_2 feed gas at 28.3 bar (410 psia) and 400 °C (consistent with O_2-ATR feed), then depressurized and purged with 68% H_2O, balance N_2 at various flow rates from 6.9 to 13.8 lpm, or 3.1 to 6.2 lbmol/h/ft^2. The f-curves are plotted in Figure 9, which again show limited sensitivity to the purge gas velocity. Also shown is a plot of the total amount of CO_2 (in standard liters; 70 °F, 1 atm) removed for each of these runs. These data form the basis for calculating the performance of the industrial SEWGS process.

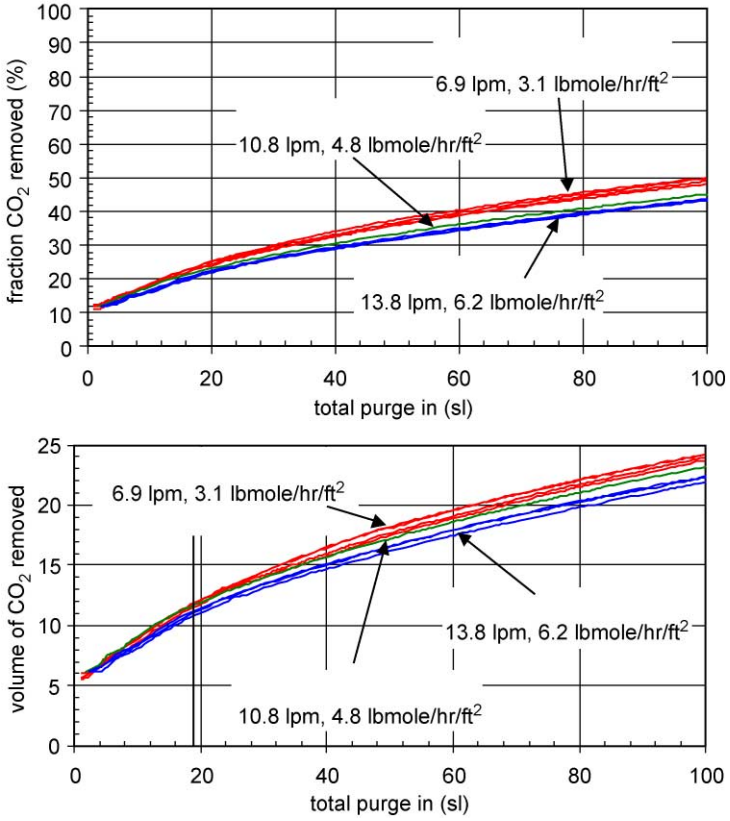

Figure 9: Plot of fraction and total standard liters of CO_2 removed during regeneration, 68% steam in purge.

Cyclic process experiments. The process test unit was operated in cyclic mode to evaluate the effective working capacity and adsorbed phase working capacity of the HTC adsorbent. The cycle consisted of a high-pressure feed step with a mixture of CO_2, H_2O, and N_2; countercurrent (and throttled) depressurization to ~1.7 bar (25 psia); countercurrent purge with a mixture of H_2O and N_2; and countercurrent

repressurization with a mixture of H_2O and N_2. The composition and flow rate of the effluent streams were continuously evaluated and used to evaluate CO_2 working capacities (amount of CO_2 removed from the feed gas per mass of adsorbent in the vessel). The adsorbent was demonstrated to be capable of removing CO_2 from the feed gas at 400–500 °C under cyclic steady-state conditions. The cyclic experiments were consistent with the trends observed with the desorption experiments—regeneration efficiency was more strongly controlled by the total amount of purge gas and was relatively insensitive to the flow rate of the purge gas at the flow rate ranges accessible by the process test unit. It was confirmed that the working capacity from the cyclic experiments can be closely estimated from the desorption curves. This forms the basis for process design via the desorption data.

A concerning observation was noted when cycles were carried out with an additional CO_2 rinse step. CO_2 accumulated on the adsorbent, and cyclic steady state was not reached even after 180 cycles. Since this is a potentially serious issue for the process, additional work is planned under rinse conditions more consistent with the industrial SEWGS process. Details of these experiments can be found in Ref. [1].

SEWGS concept demonstration. A key objective in this program was to demonstrate the concept of the SEWGS process in the process test unit. We wanted to show that simulated syngas could be fed to a column containing the CO_2 adsorbent and shift catalyst, and decarbonized hydrogen product could be obtained as a product gas. The experimental plan was to investigate individual reaction breakthrough/regeneration steps first, and then run the unit cyclically. Two feed gas mixtures were used, one consistent with O_2-ATR syngas (11.2% CO, 20.7% CO_2, balance H_2) and the other with air-ATR syngas (6.4% CO, 13.4% CO_2, 38.1% H_2, balance N_2).

Reaction breakthrough tests. The first experiment was run as a baseline test of the system, to confirm that the catalyst would not impart any dynamic SEWGS effects on the results (e.g. CO_2 removal via coking or other mechanisms would yield similar effects as CO_2 removal on an adsorbent). Reduced catalyst was exposed to 9.3% CO, 17.4% CO_2, 57.5% H_2 and 15.8% H_2O at a space velocity of 1720 h^{-1}, 400 °C, 400 psig. The composition of the effluent gas is illustrated in Figure 10. All carbon components, CO, CO_2, and CH_4, exit the reactor once the void gas has been pushed out, designated by the vertical red line in Figure 10. There is no holdup of CO_2 in the column associated with the catalyst or ceramic balls. The CO level indicates that the effluent gas is very close to the equilibrium limit. The methane in the product gas is likely formed from CO and H_2 via the methanation reaction, either catalyzed by the reactor walls or the shift catalyst. The oscillations in the mole fractions are due to small fluctuations in the feed gas steam generator heating system.

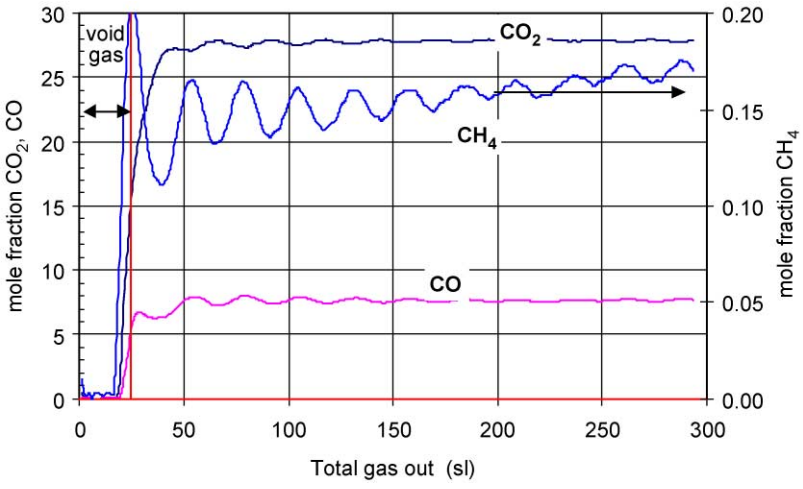

Figure 10: Effluent gas composition (dry) for a reaction breakthrough experiment with catalyst/ceramic balls; 400 °C, 400 psia.

The next set of reaction breakthrough experiments were conducted with a mixture of catalyst and the HTC adsorbent. The feed gas was the same as above, and a 5:1 volumetric ratio of HTC adsorbent to catalyst was used (0.47 g catalyst/g adsorbent). The effluent gas mole fractions are plotted in Figure 11. In this case, only CH_4 breaks through once the void gas is displaced. Carbon dioxide is retained by the adsorbent, and does not breakthrough until 110 sl of effluent gas has been produced. The removal of CO_2 drives the WGS reaction to completion, so the CO mole fraction exhibits similar behavior. The first 110 sl of effluent gas contain the H_2 from the feed gas, H_2 produced from the reaction, the small amount of CH_4 produced via methanation, and the initial amount of pressurization gas in the bed before the run. Subtracting out the latter indicates that 90 sl of decarbonized H_2 product is obtained in the product gas. Once the CO_2 and CO breakthrough, they stabilize to similar levels measured during the catalyst-only experiments. Temperature increases of ~35 °C were observed along the reactor length as the CO_2 front traveled down the bed. Heat is generated both from the WGS reaction and CO_2 adsorption.

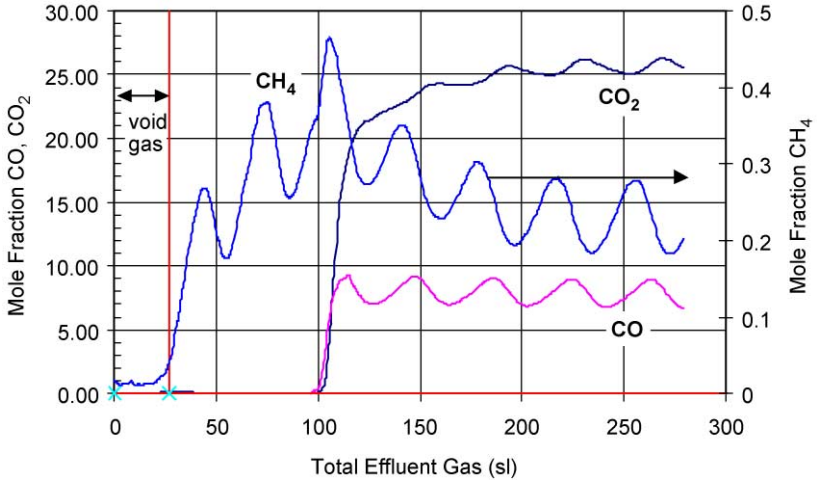

Figure 11: Effluent gas composition (dry) for a reaction breakthrough experiment with catalyst/HTC adsorbent and O_2-ATR feed; 400 °C, 400 psia.

A similar experiment was carried out for air-ATR feed gas (5.4% CO, 11.3% CO_2, 32.1% H_2, 35.5% N_2, 15.8% H_2O). The effluent gas mole fraction data are plotted in Figure 12. Once again, the CO_2 and CO are retained by the adsorbent, and 130 sl of decarbonized product gas is produced (excluding pressurization gas and disregarding low level of CH_4). A lower temperature peak of 25 °C was observed in these experiments.

These experiments demonstrate the basic sorption enhanced reaction concept for the WGS reaction.

The beds were regenerated after these reaction breakthrough steps via the typical procedure (depressurization, purge with 6.9 slpm of 68% steam in N_2). The regeneration data were consistent with adsorbent-only regeneration experiments—the catalyst has no effect on desorption of CO_2 from the adsorbent. The total amount of CO_2 removed by the adsorbent during the reaction breakthrough steps can be evaluated from Figures 11 and 12, along with other runs that are not shown. The measured capacities from the reaction experiments plotted in the isotherm plot of Figure 13 are in great agreement with the adsorbent-only isotherm data at 400 °C, indicating that the adsorbent in the bed is fully utilized and the reaction breakthrough behavior can be based on the adsorbent-only capacity data. This is the approach taken in design of the industrial SEWGS process.

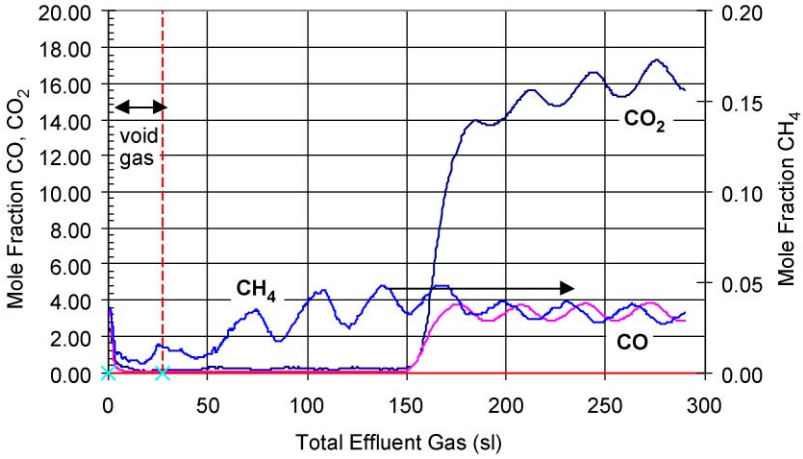

Figure 12: Effluent gas composition (dry) for a reaction breakthrough experiment with catalyst/HTC adsorbent and O_2-ATR feed; 400 °C, 400 psia.

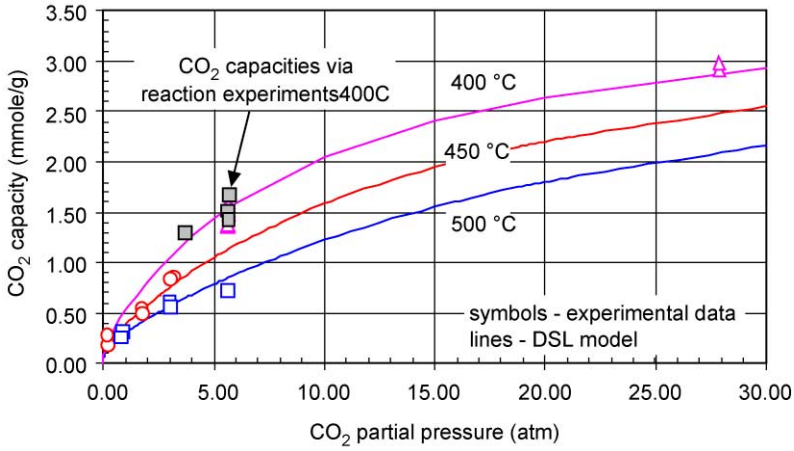

Figure 13: Comparison of CO_2 capacities obtained via reaction breakthrough experiments with CO_2/HTC isotherm.

Cyclic reaction experiments with catalyst and adsorbent. A cyclic reaction experiment was carried out with the same catalyst/adsorbent bed at 400 °C. The cycle consisted of 310 s of feed (O_2-ATR feed gas) at 400 psia, countercurrent depressurization, 135 s of countercurrent purge with 6.0 slpm of 68% steam in N_2, and repressurization to 400 psi with 68% steam, 0.6% H_2 in N_2. The feed gas contained 11.2% CO and 20.7% CO_2 on a dry basis. Cycle data are presented in Figure 14 which shows that the effluent levels, on a dry basis, appear to have stabilized after 20 cycles to 4.8% CO_2, 0.15% CH_4, and 1.5% CO (these values were calculated without the pressurization gas). Thus, the carbon content of the feed gas has been reduced by a factor of five. Operation with slightly lower feed time or flow rate would yield lower CO/CO_2 in the product. This data set indicates that the adsorbent/catalyst system can be operated cyclically and used to remove CO_2 and CO from the feed gas.

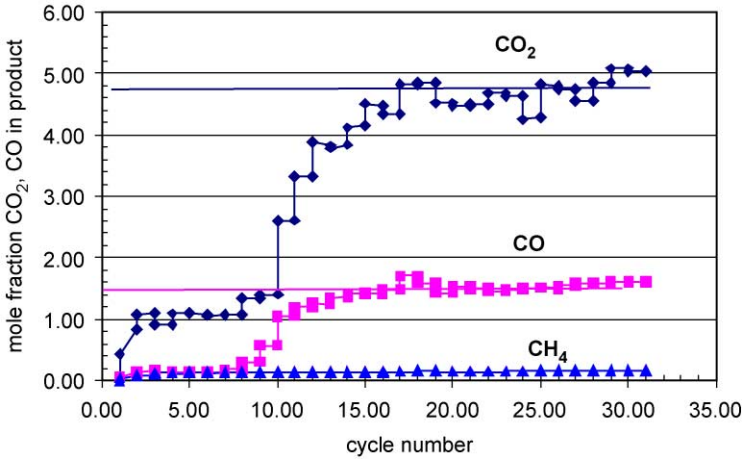

Figure 14: Product gas mole fraction of CO, CH_4 and CO_2 during reaction cycles with O_2-ATR feed gas.

SEWGS process design

The SEWGS process cycle considered for all scenarios is the RINSE/EQ cycle, illustrated in Figure 2. Seven vessels are needed to accommodate all of the steps, and the total cycle time is 4.67 min. Two of the beds receive feed gas at any particular time. The sequence of steps is configured so a constant feed and product flow is attained.

Initial design plans were to use the modified dynamic simulator to scale-up the experimental data to industrial conditions. Unfortunately, the linear driving force model was incapable of describing the desorption data obtained with the HTC. We therefore took a more experimental approach in estimating process performance.

The design working capacity of the HTC adsorbent was based on measured CO_2 desorption curves for 68% steam purge at 400 °C and a G rate of 3.1 lbmol/h/ft^2. Selecting the amount of purge gas (mmol/g adsorbent) defines the working capacity of the adsorbent via these curves (Figure 9). This approach was tested by comparing the results with cyclic experiments and the agreement was very good. The SEWGS feed gas was O_2-ATR or air-ATR syngas defined from ASPEN simulations (described in a later section). The CO_2 level of these streams is consistent with the CO_2 content of the saturation gas used in the desorption experiments. A CO conversion of 95% is assumed, and 100% recovery of nonadsorbing gas. The product gas composition and amount is evaluated from mass balance, and the product temperature is determined assuming all of the reaction heat exits with the product.

The biggest uncertainty in the above CO_2 working capacity is what impact the addition of the CO_2 rinse step will have on performance. Simulations suggest that the working capacity will be reduced by approximately 50%, which has been incorporated in the design. This modified working capacity is then used to evaluate the size of the reactors. The steam purge requirement is fed to the ASPEN simulator for integration into the rest of the power generation process.

The required catalyst amount for each SEWGS vessel was estimated from nonisothermal reaction calculations using kinetic rate expressions for the forward and reverse reaction on HTS catalyst (taken from Ref. [4]). The rate of reaction in the SEWGS case is enhanced by the removal of CO_2 on the adsorbent, which substantially reduces the backward reaction rate. The SEWGS activity estimates were made by setting the CO_2 gas phase concentration to zero, which essentially provides measure of the forward rate of reaction. The total calculated catalyst volume needed for this conversion was multiplied by four to account

for the nonstationary mass transfer/reaction zone. These calculations yield adsorbent to catalyst volume ratios of 5:1, which is consistent with the ratio used in the reaction experiments.

Assumptions made during design of the SEWGS process units are listed in Table 5.

TABLE 5
MAJOR ASSUMPTIONS IN SEWGS DESIGN

Feed temperature, 400 °C	Vessel ID, 12 ft
Feed pressure, 390 psia	Feed flow/rinse flow, 4.7
Nonadsorbing gas recovery in product, 100%	Adsorbent bulk density, 37 lb/ft^3
CO conversion, 95%	Catalyst bulk density, 70 lb/ft^3
7 beds/train	Rinse step derate of working capacity, 50%
4.67 min total cycle time	Total void fraction, 0.74
Purge requirement	
0.75 mmol/g ads for air-ATR	Adsorbent/catalyst volume, 5–5.3:1
0.85 mmol/g ads for O_2-ATR	
Adsorbed phase working capacity	
0.25 mmol/g ads for air-ATR	
0.32 mmol/g ads for O_2-ATR	

Power Generation Process Development

Norcap scenario

In this scenario, the goal is to develop a process for producing power (350 MW) with drastically reduced CO_2 emissions. A gas turbine combined cycle incorporating the General Electric 9FA was utilized. It was decided to study both O_2 and air-ATR flowsheets for this scenario—although air-ATR gives higher efficiencies, the O_2-ATR process gives lower costs due to smaller equipment sizes since the nitrogen has been separated out in the ASU. The option of using a sidedraw from the gas turbine compressor was excluded.

Process flow diagrams for both cases are shown in Figures 15 and 16. Heat and mass balance and equipment lists can be found in the report of Allam et al. [1], along with more specific details of the simulation work.

Gas turbine modeling. Models for the General Electric 9FA gas turbine were generated to allow extrapolation of performance to H_2-rich fuel gas with and without diluents. A natural gas fired 9FA turbine producing 226 MW under ISO conditions was modeled with Aspen, and machine efficiencies were adjusted until the model predicted the performance data quoted in GE literature. The power output of the gas turbine can be increased until it reaches a level of 290 MW which is imposed by mechanical limits of the machine.

The air flow rate through the gas turbine compressor section was back-calculated from gas turbine data published by GE, and held constant in future simulations. There is an air bleed flow of 10% modeled to simulate the bypass flow around the combustion section of the gas turbine for use as blade cooling air. Fuel flow to the turbine combustion section, and hence natural gas flow to the ATR, was adjusted to yield a gas turbine combustor exit temperature of 1288 °C. Since the gas turbine compressor flow rate and compressor power are constant, the net total gas turbine power is governed by the flows entering the combustion chamber and passing through the expander section. To achieve the 290 MW power, a diluent must be added to the combustion chamber to boost the power generated by the gas turbine expander. In these cases, the diluent is either steam or, for the O_2-ATR case, a combination of steam and nitrogen from the ASU.

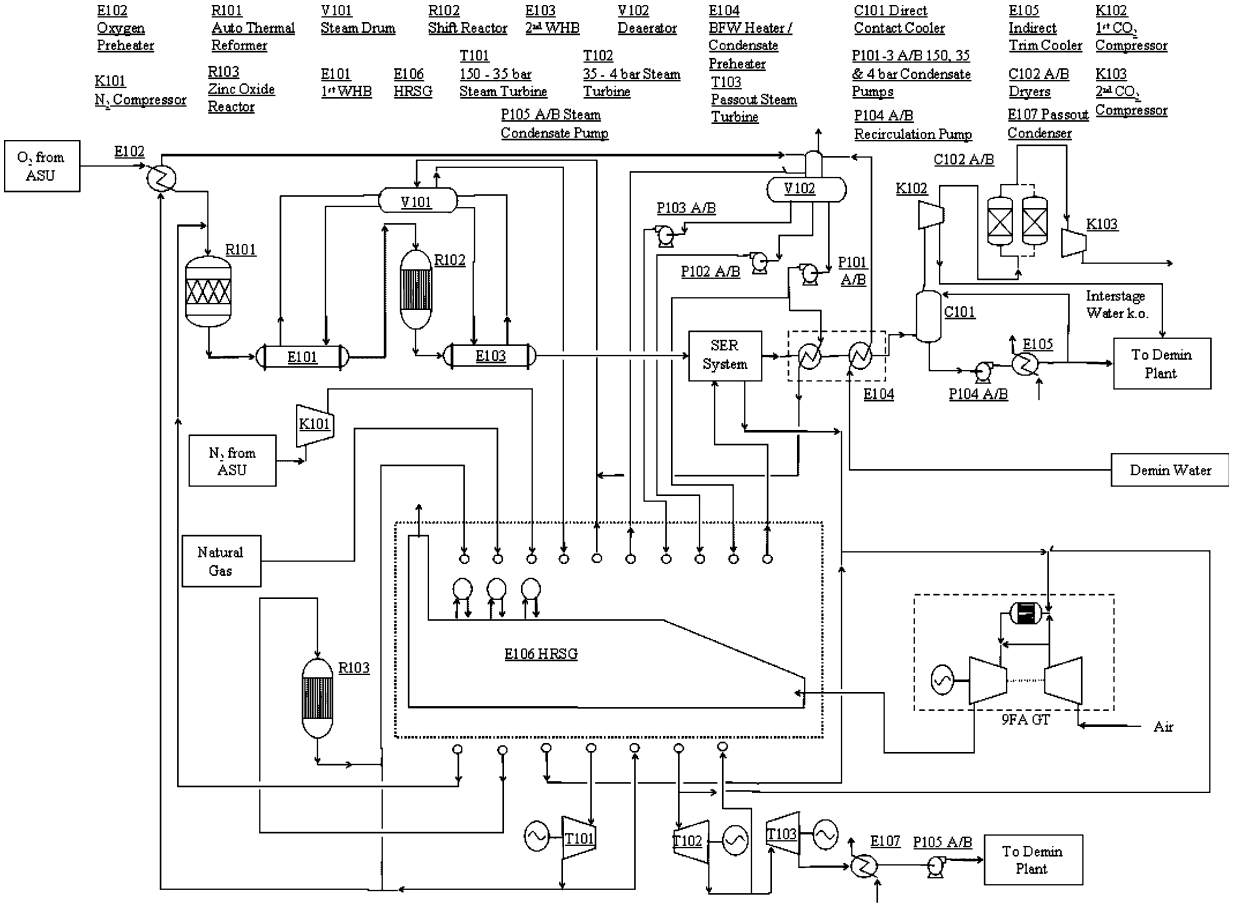

Figure 15: PFD of the Norcap scenario O_2-ATR process.

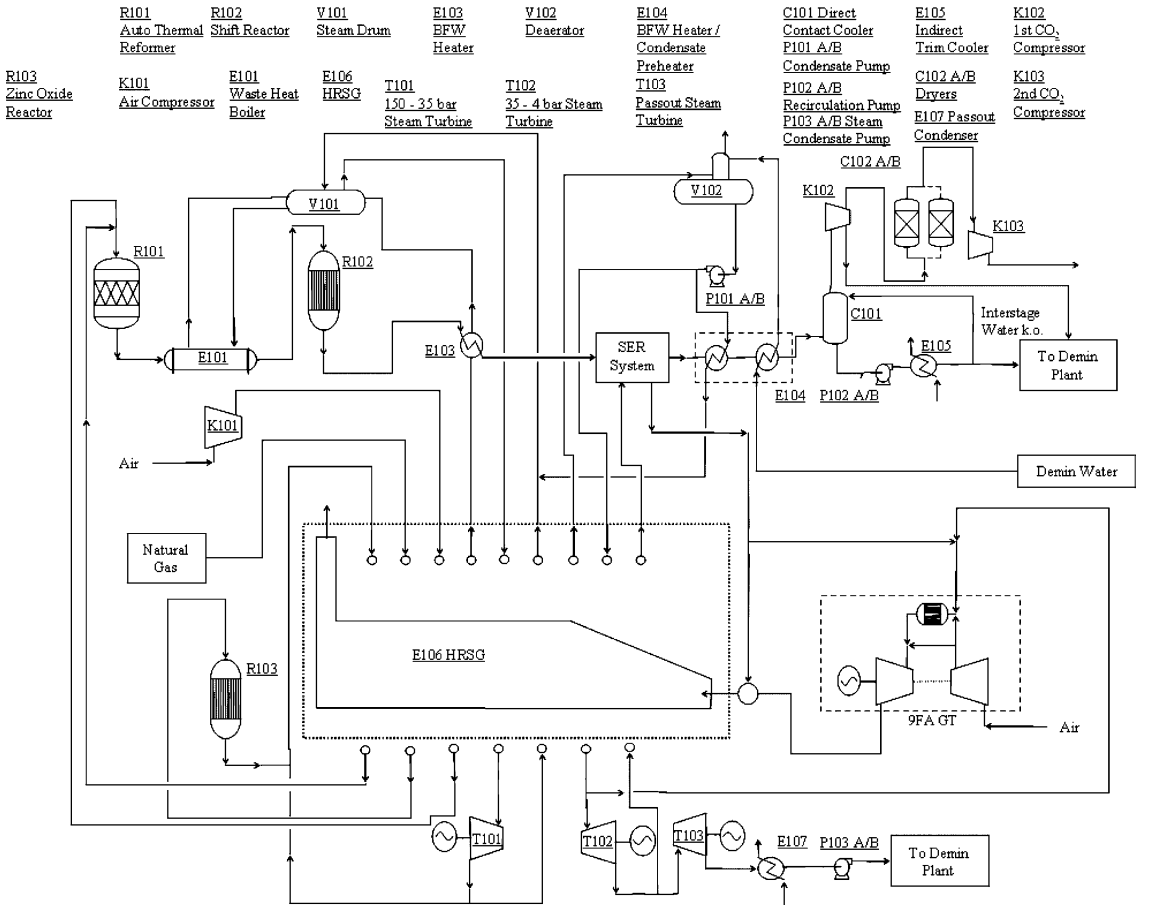

Figure 16: PFD of the Norcap scenario air-ATR process.

One important effect of the use of steam and nitrogen diluent is to limit the NO_x levels in the gas turbine exhaust. Figure 17 shows the effect of fuel calorific value, which is affected by nitrogen or steam dilution of the nitrogen, on the NO_x emission levels (GE data from Ref. [5]). Since 20 ppm is considered to be the limit, we aim to have a calorific value less then 6 MJ/Nm^3.

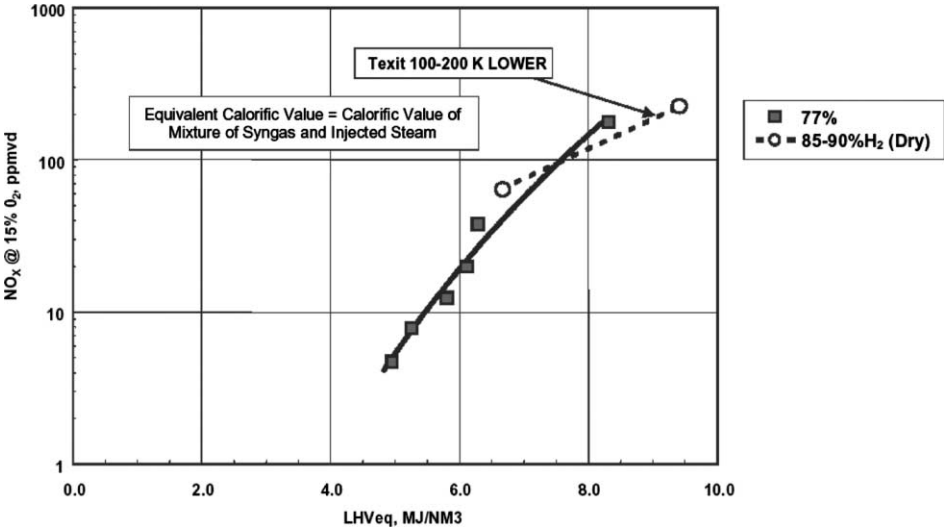

Figure 17: NO_x versus equivalent calorific value for several fuel compositions; taken from Ref. [5].

Flue gas leaves the exhaust of the gas turbine expander at around 590 °C and 1.05 bara. In the air-ATR case, a duct heater is used to boost this temperature to 696 °C with some of the hydrogen fuel in order to accommodate the extra steam generation in the WHB compared to the O_2-ATR case. The heat from this stream is then removed to produce more power in the heat recovery steam generation section (HRSG E106). The flue gas finally leaves the HRSG and is vented at a temperature of around 115 °C in the air-ATR case and 132 °C in the O_2-ATR case.

Steam cogeneration. The cogeneration section is modeled as a three pressure level re-heat cycle. The air and O_2-ATR cases are slightly different in this area. In the O_2-ATR case make-up water is supplied by pumping to three pressure levels from the de-aerator V102: 4, 35, 150 bara. These make-up streams are vaporized and superheated in the HRSG, and for the 150 bar steam in the ATR WHB E101, and provide the "3-level" pinched cooling curve in the HRSG heat exchanger that maximizes the thermal efficiency of the system. The majority of the steam is raised as 150 bar steam in the WHB. In the air-ATR case steam is only raised at 150 bar and only in the WHB E101; no steam is raised in the HRSG, which only carries out preheating and superheating.

In both cases, the superheated streams are let down in multistage steam turbines, T101, T102 and T103, to the next lower pressure level (e.g. 150 bar let down to 35 bar) and then reheated, mixed with vaporized make-up water in the O_2-ATR case, and passed through the next steam turbine in the series. The final pass out turbine, T103, with an inlet pressure of 4 bara, has an outlet pressure of 0.03 bara. This is fixed by the seawater temperature, permitted temperature rise and the approach temperature in the condenser E107. The 0.03 bara water can then be pumped back up to pressure and recycled to the make-up water streams.

The make up water flow rates are varied by the process modeling (Aspen) optimizer to maximize the power output from the steam turbines without crossing the HRSG cooling curves. A 20 °C minimum temperature approach is allowed in the HRSG.

Heat integration. As well as providing heat to power the steam cycle, the HRSG can also provide preheating duty for the H_2 process plant feeds such as the natural gas and the air. Steam for the reforming processes can also be taken from the cogen cycle. Significant high-value heat is also available at other points in the process such as after the reformer in the WHB E101, after the shift reactor, R102, and after the SEWGS system. In both process schemes, the recovery of all this available heat in the most efficient way is the focus of the modeling.

The most efficient configurations may often involve partially heating a stream at different points in the process until the stream is up to the required temperature. Examples might include preheating and superheating of a water stream in the HRSG and providing the vaporization duty for the same stream in the WHB. Any steam that is produced in the WHBs will be fed back into the cogeneration cycle at the equivalent pressure and temperature level to produce more power.

By moving more of the vaporization load out of the HRSG, the HRSG cooling curves end up becoming very close and approximately parallel. For instance, there is more heat available in the WHB E101 of the air-ATR case due to the nitrogen content of the process gas compared with the O_2-ATR case. The WHB is specified only to be used to evaporate 150 bara water. It can vaporize a very large amount of 150 bara water, which must all be preheated and superheated in the HRSG. This places a very large sensible heat duty demand on the HRSG and there is no excess heat available to raise 4, 35 and 150 bar steam. In fact a duct heater is required to open the cooling curve and allow the preheating of all of the BFW to E101 and the superheating of all the steam that is raised in E101.

In the O_2-ATR case where the vaporization load of the WHB is far less, there is a much lower sensible heat duty demand on the HRSG (less preheating and superheating is required). Vaporizing process water at the different pressure levels and then expanding in a steam turbine system uses the excess heat most efficiently.

SEWGS system. The SEWGS system was modeled in ASPEN using a "Stoichiometric Reactor" block followed by a separator block. The only reaction specified in the SEWGS block was the water gas shift reaction and this was specified to consume 95% of the feed CO. The separator block removes only CO_2 from the product stream, simulating adsorption and desorption of the CO_2. Only enough CO_2 is separated to give a 90% recovery of carbon. Steam, at 4 bar and 400 °C is used to regenerate the catalyst/adsorbent bed. The amount of steam required was taken as 1.8 mol of steam per mole of CO_2 removed from results of the experimental work. The heat of reaction is assumed to leave with the hydrogen-rich stream, consistent with dynamic simulations.

Two SEWGS process designs, for air-ATR and O_2-ATR, were developed for the Norcap scenario as per the experimental data-based design procedure described previously. Each required four separate trains of vessels to accommodate the feed flow. Relevant details of the designs are listed in Table 6.

Autothermal reforming with air. The ATR reformer, modeled as a "Reformer Reactor" block, is fed with natural gas, air and steam. The air rate is adjusted to achieve a 1050 °C outlet temperature. Steam for the ATR is taken directly from the steam cogeneration cycle and mixed with preheated, desulfurized natural gas. A steam-to-carbon ratio of 1.1 is used. A WHB E101 is used to cool the syngas to 350 °C by raising 150 bar steam. This cooled syngas then passes to the HTS reactor R102 where CO and water are shifted to CO_2 and hydrogen. The product is cooled to 400 °C in E103 and passed to the SEWGS.

Autothermal reforming with O_2. The O_2-ATR cycle is specified to have the same ATR outlet temperature as the air-ATR; 1050 °C. The steam-to-carbon ratio is kept at 1.1 and natural gas and steam are preheated as above. Nitrogen from the ASU is compressed in K101 and preheated in the HRSG E106 and is used as a

TABLE 6
SUMMARY OF SEWGS DESIGNS

	Norcap air-ATR	**Norcap O_2-ATR**	**Alaska O_2-ATR**
Number of trains	4	4	6
Total flow (kmol/h)	25,767	14,060	26,496
Feed gas (mol%)			
CH_4	0.1	0.5	0.3
CO	5.0	9.6	9.2
H_2	35.9	57.3	54.5
CO_2	11.4	16.2	17.6
H_2O	10.3	15.6	17.4
Inert	37.2	0.9	0.9
Product gas (mol)			
CH_4	0.1	0.6	0.5
CO	0.3	0.6	0.6
H_2	47.7	86.9	83.8
CO_2	1.5	2.2	2.5
H_2O	6.6	8.5	11.4
N_2	43.7	1.1	1.2
Vessel length (ft)	39	25	32
Vessel diameter (ft)	12	12	12
Total ads needed (lbs)	3,844,563	2,413,751	4,652,324
Total cat needed (ft^3)	19,742	13,047	25,148
Feed G-rate ($lbmol/h/ft^2$)	62.7	34.6	43.4
Estimated feed pressure drop, psi	0.3	0.1	0.2
Purge G-rate ($lbmol/h/ft^2$)	40.8	29.5	38.2
Estimated feed pressure drop (psi)	16.0	7.9	14.3
Adiabatic T rise (C)	68.4	147.7	142.6
CO_2/rinse flows (kgmol/h)			
CO_2 product flow, dry, without rinse stream	3,828	3,319	6,486
Average CO_2 rinse flow	5,482	2,992	5,637

diluent in the gas turbine combustor. After all the available nitrogen is added, a small amount of extra steam is required to make the power up to the 290 MW.

Results. A summary of the performance of the two processes for the Norcap scenario is shown in Tables 7 and 8. The O_2-ATR system yields a thermal efficiency of 47.3% and a net export power of 361 MW after taking into account the power for the pumps, the ASU, the nitrogen compressor and the CO_2 compressor. The air-ATR achieves higher efficiency at 48.3% and produces more power, 425 MW. This is because more steam is generated in the air-ATR WHBs. More fuel is required, but efficiency is still higher. The higher amount of fuel required for the air-ATR case, mostly due to the requirement for duct heating, leads to the capture of more CO_2 from the system.

In the preliminary study, it was shown that air-ATR systems have higher thermal efficiency than O_2-ATR systems and this has been confirmed. However, the fact that the air-ATR system processes all of the nitrogen associated with the air feed means that the hydrogen generation and purification equipment sizes are much bigger and more costly. A detailed cost estimate is required to evaluate both alternatives.

TABLE 7
PERFORMANCE SUMMARY FOR NORCAP SCENARIO, O_2-ATR WITH SEWGS

	Units	Value		
GT power output	MW	290.00		
Steam turbine output	MW	130.12		
Total	MW	420.12		
Contained oxygen feed	kg/h	63,417		
	tonne/day	1,522		
	kmol/h	1,982		
ASU power	MW	27.99		
CO_2 compressor power	MW	12.03		
N_2 compressor power	MW	16.61		
BFW pumps power	MW	2.13		
Recirculation Pump	MW	0.13		
Total power	MW	58.89		
Export Power	MW	361.23		
Total natural gas fuel	kg/h	60,455		
	kmol/h	2,915		
	MW, LHV	763.75[a]		
Thermal efficiency, based on LHV		47.30%		
Cooling requirements				
Glycol… assuming 19 °C inlet and 34 °C outlet temperatures	C_p = 3263 J/kg °C			
ASU	MW	29.46	tonne/h	2,166.77
CO_2 inter/after cooling	MW	22.86	tonne/h	1,681.16
N_2 intercooling	MW	12.53	tonne/h	921.63
Total	MW	64.84	tonne/h	4,769.57
Seawater… assuming 11 °C inlet and 21 °C outlet temperatures				
E105—indirect cooler	MW	44.87	tonne/h	3,688.90
E107—steam condenser	MW	151.29	tonne/h	12,437.61
Total	MW	196.16	tonne/h	16,126.51
Makeup water for Demin plant	tonne/h	45.54		
Carbon dioxide captured	Million tonnes/year	1.28[b]		

[a] HHV = 842.15 MW.
[b] 8760 h/year.

Alaskan scenario

The O_2-ATR process was chosen for the decarbonization of fuel for the Alaska scenario, and it is similar to the Norcap scenario O_2-ATR. In the Alaska case, however, only enough power is generated to satisfy the ASU, CO_2 compression system and auxiliaries of the fuel generation process. To that end, the process is integrated with only a 85.4 MW 7EA gas turbine, providing much less opportunity for process heat recovery/integration from the gas turbine exhaust.

A process flow diagram for the Alaskan O_2-ATR system is illustrated in Figure 18. Heat and mass balance and equipment lists can be found in the report of Allam et al. [1].

Alaskan gas turbines. The aim of this scenario was to repower 11 open cycle gas turbines, described in Table 1, with hydrogen fuel. All of the available nitrogen from the ASU was used to dilute the hydrogen to keep NO_x levels at 20 ppm per GE literature.

TABLE 8
PERFORMANCE SUMMARY FOR NORCAP SCENARIO, AIR-ATR WITH SEWGS

	Units	Value		
GT power output	MW	289.99		
Steam turbine output	MW	188.54		
Total	MW	478.54		
CO_2 compressor power	MW	13.87		
Air compressor power	MW	36.54		
BFW pumps power	MW	2.94		
Recirculation pump	MW	0.13		
Total power	MW	53.49		
Export power	MW	425.05		
Total natural gas fuel	kg/h	69,714		
	kmol/h	3,361		
	MW, LHV	880.73[a]		
Thermal efficiency, based on LHV		48.26%		
Cooling requirements				
Glycol… assuming 19 °C inlet and 34 °C outlet temperatures	C_p = 3263 J/kg °C			
CO_2 inter/after cooling	MW	26.36	tonne/h	1,938.71
Air intercooling	MW	31.17	tonne/h	2,292.66
Total	MW	57.53	tonne/h	4,231.37
Seawater… assuming 11 °C inlet and 21 °C outlet temperatures				
E105—indirect cooler	MW	46.01	tonne/h	3,783.24
E107—steam condenser	MW	216.61	tonne/h	17,806.76
Total	MW	262.62	tonne/h	21,590.00
Makeup water for Demin plant	tonne/h	86.51		
Carbon dioxide captured	Million tonnes/year	1.47[b]		

[a] HHV = 971.14 MW.
[b] 8760 h/year.

Due to lack of information on hydrogen-powered turbines, we assumed that the power of each gas turbine fueled with natural gas remains the same when fueled with hydrogen, as well as the temperature from the combustor. In essence, the compressor section has been "turned down" so as not to exceed the power output achieved with natural gas. The 11 turbines were then modeled to determine how much hydrogen fuel is required from the O_2-ATR/SEWGS process.

The hydrogen production/CO_2 removal process is similar to the Norcap O_2-ATR process.

SEWGS process. An SEWGS design for O_2-ATR syngas was developed for the Alaskan scenario as per the experimental data-based design procedure described previously. A total of six trains were necessary to handle the higher feed flow rate. Results are also listed in Table 6.

To aid in fabrication, the SEWGS process unit will be packaged into modules for this scenario. A layout utilizing three modules is illustrated in Figure 19 (a two-skid approach has also been developed). Two process trains are packaged per module, with a central skid area for controls/piping. The centrally located module houses a shared assembly of blowdown tanks and associated piping.

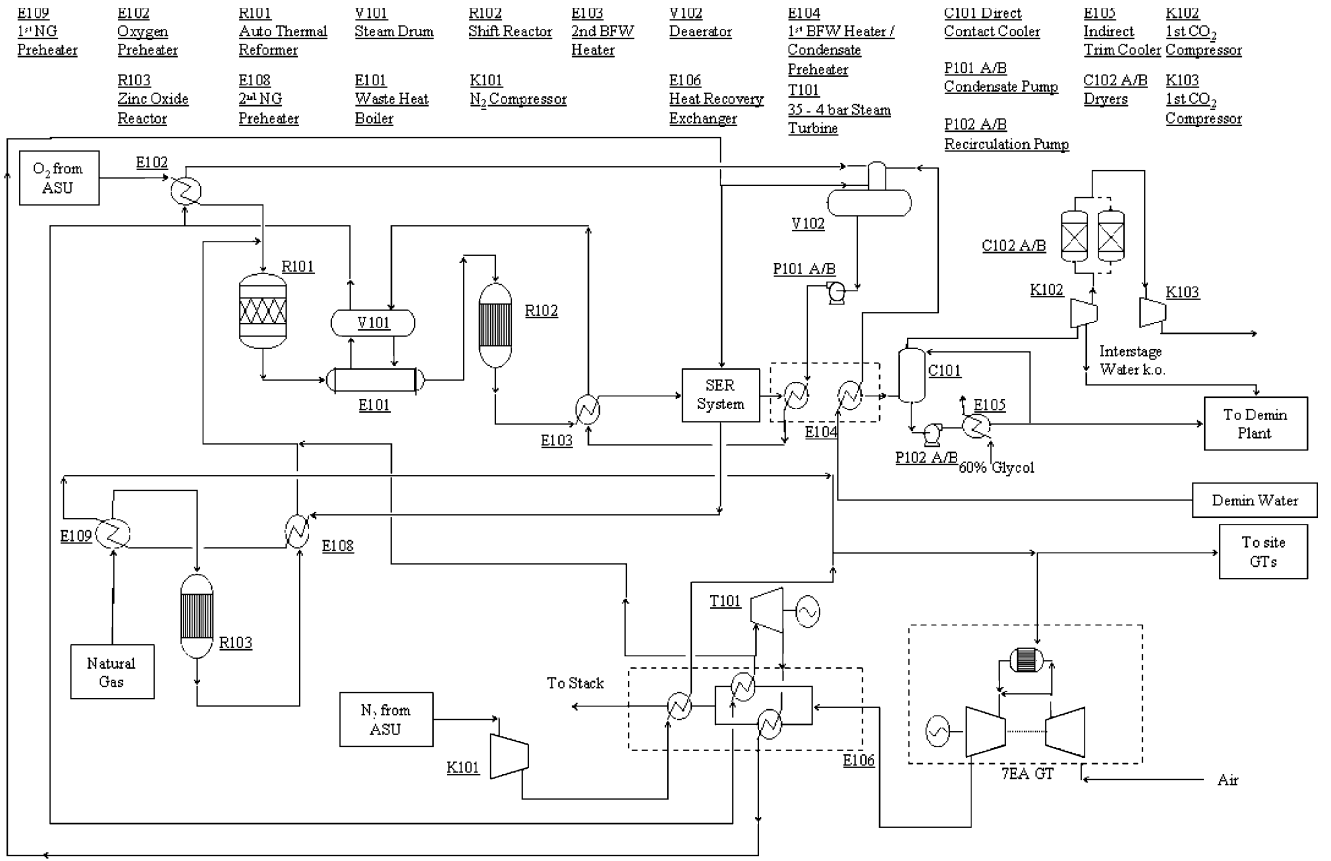

Figure 18: Alaska scenario O_2-ATR PFD.

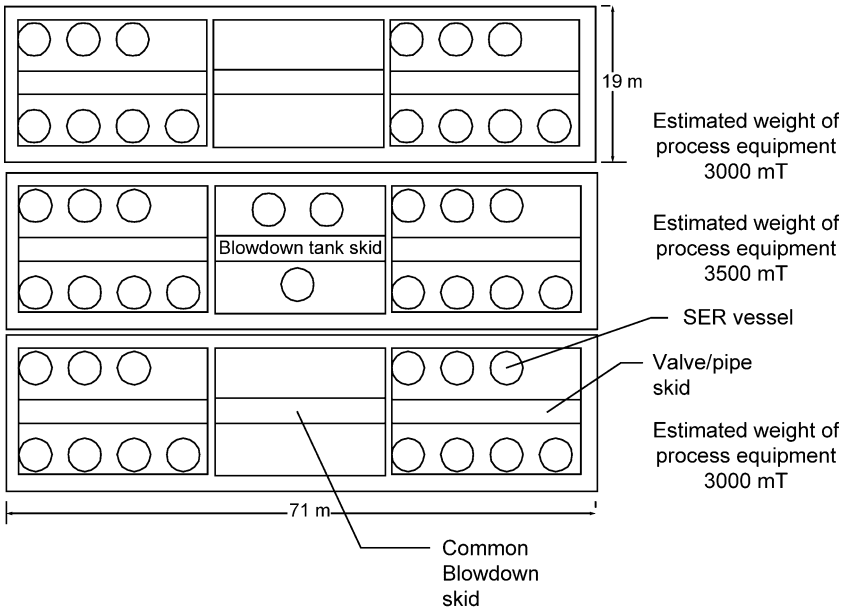

Figure 19: Proposed layout for SEWGS process unit in Alaskan modules.

Results. It is difficult to judge the performance of this system by efficiency. The 11 distributed gas turbines are open cycle. Since no export power was desirable, the gas turbine integrated with this process cycle is smaller than desired for optimal process integration. The optimum solution, from an energy efficiency point of view, is to retrofit HRSGs onto the existing open cycle gas turbines, but this was ruled out on the basis of cost and practicality.

The results in Table 9 show that 137,259 kg/h of natural gas is required compared to the sum of 108,351 kg/h when firing with natural gas. However, this includes the fuel to power the compression of the CO_2 to 220 barg for EOR, and 2.5 million tonnes/year of CO_2 are captured from this process.

The entire fuel generation process can be housed in four, and possibly three, modules. An isometric illustration of the former system is attached in Figure 20.

Economic Evaluation

Capital costs associated with the SEWGS processes were evaluated at Air Products and are listed in Table 10. Our experience in building and operating world-scale hydrogen PSA units served as the foundation for these estimates, with various cost adders associated with the unique service conditions (high temperature) of the SEWGS process. The results show that the air-ATR equipment is more costly than for O_2-ATR. The cost of adsorbent and catalyst represents roughly 40% of the total installed cost. Vessel costs are the most significant component of mechanical equipment.

The overall costs for the complete power generation processes (Alaskan and Norcap scenarios) were evaluated by independent CCP-funded cost evaluators based on Air Products equipment specifications. The results show favorable economics for the SEWGS-based processes compared to other technologies.

TABLE 9
PERFORMANCE SUMMARY FOR ALASKA SCENARIO, O_2-ATR WITH SEWGS

	Units	Value
GT power output	MW	85.40
Steam turbine output	MW	28.92
Total	MW	114.31
Contained oxygen feed	kg/h	124,174
	tonne/day	2980
	kmol/h	3880
ASU power	MW	54.80
CO_2 compressor power	MW	25.99
N_2 compressor power	MW	32.48
BFW pump power	MW	0.41
Recirculation pump	MW	0.09
Total power	MW	113.68
Export power	MW	0.64
Total natural gas fuel	kg/h	137,259
	kmol/h	6554
Glycol duty (assumed 24 °C supply and 43 °C return)		
ASU	MW	57.68
Trim cooler	MW	138.70
CO_2 inter/after cooling	MW	24.66
N_2 intercooling	MW	23.99
Total	MW	245.03
	tonne/h	16,030.99
Makeup water for Demin plant	tonne/h	130.52
Carbon dioxide captured (8760 h/year)	million tonnes/year	2.5

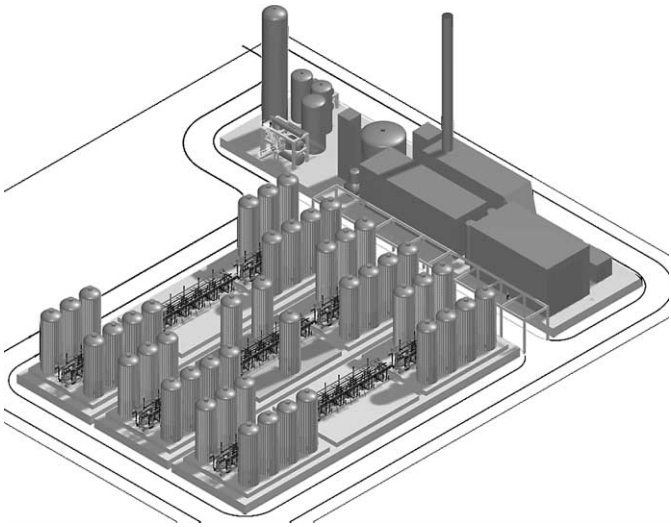

Figure 20: Layout drawing showing entire SEWGS system, excluding ASU.

TABLE 10
SUMMARY OF COSTS FOR SEWGS PROCESSES

	Cost ($MM)		
	Norcap air-ATR	**Norcap O_2-ATR**	**Alaska O_2-ATR**
Valves	3.71	3.23	4.84
Valve skidding	6.08	5.58	8.37
Vessels	10.72	7.48	13.65
Purge tank	1.31	1.31	1.31
Manual valves	0.12	0.12	0.18
Transmitters/analyzers	0.12	0.12	0.18
Installation, 4 trains	2.00	2.00	3.00
Direct cost	24.06	19.84	31.53
Engineering	1.20	0.99	1.05
Administration	0.72	0.60	0.63
Test	0.48	0.40	0.63
Contingency	6.25	5.16	8.20
Ads/cat	19.33	12.26	23.64
Loading	0.40	0.40	0.60
Total	52.44	39.65	66.28

CONCLUSIONS

Power generation process designs have been generated for the Norcap and Alaskan scenarios utilizing SEWGS fuel gas decarbonization. The SEWGS processes use HTC as a high-temperature CO_2 adsorbent. Economic evaluations indicate that this approach has potential for clean power production with CO_2 recovery for sequestration.

The performance of the K_2CO_3/HTC adsorbent (HTC) has been evaluated in the process test unit. The CO_2 adsorption isotherm has been determined and fit with a theoretical model. It exhibits a relatively linear shape. The temperature dependence of the CO_2 capacities is as expected and characterized by a 10 kcal/mol heat of adsorption. The adsorption mass transfer rate is fast, characterized by a mass transfer coefficient of at least 0.1 s^{-1}. The desorption mass transfer coefficient is lower, but lack of consistency of the model with experimental data obtained at various gas flow rates makes it impossible to assign a mass transfer coefficient value. Desorption of CO_2 from the HTC adsorbent is more efficient when the steam content of the purge gas is increased.

The SEWGS concept was demonstrated with a vessel packed with HTC and HTS catalyst. With no adsorbent, CO and CO_2 breakthrough once the void gases are displaced. When adsorbent is added, the CO_2 breakthrough is delayed, and the removal of CO_2 drives the CO to insignificant levels. Decarbonized product gas containing feed H_2 and N_2 and additional H_2 formed via the reaction is produced at reaction pressure and temperature. A cyclic experiment was conducted, which demonstrated that a stable product gas can be formed with 5 times less $CO + CO_2$ than in the feed.

CO_2 was found to accumulate on the adsorbent when high-pressure CO_2 rinse steps were utilized. Cyclic steady state was not reached even after 180 cycles. Since this is a potentially serious issue for the process, additional work should be carried out under conditions more consistent with the SEWGS process.

The adsorption process model does not describe the impact of purge flow rate on the observed desorption data. Namely, experimental data indicate that desorption of CO_2 from HTC is rate limited, but the

desorption process is not very sensitive to purge flow rate. Cyclic experiments also support this conclusion. An alternative approach has been taken to generate an approximate SEWGS process design from the experimental data.

RECOMMENDATIONS

Future development work will focus on key issues that can be addressed with the current process test unit, followed by complete demonstration of the SEWGS process in a multi-bed process development unit. In the first phase, the existing process test unit will be used to investigate the impact of CO_2 accumulation on the adsorbent during continuous rinse cycles, evaluate the effect of higher feed/purge gas flow rates on process performance, determine the source of methane production during reactive SEWGS feed steps, develop models of the CO_2 adsorption/desorption process that describe the experimental data, and conduct rigorous and detailed mechanical evaluations for vessels, piping, valves. In the second phase of work, an automated, multi-bed test unit will be built of sufficient size (bed length) to permit direct demonstration of cyclic process performance (including all steps of the RINSE/EQ process cycle).

ACKNOWLEDGEMENTS

This work was funded by the CO_2 Capture Project along with the US Department of Energy under the program "CO_2 Capture Project: An Integrated, Collaborative Technology Development Project for Next Generation CO_2 Separation, Capture and Geologic Storage", under Award No. DE-FC26-01NT41145.

REFERENCES

1. R.J. Allam, R.L. Chiang, J.R. Hufton, R. Quinn, E.L. Weist, V. White, CO_2 Capture Project—an integrated, collaborative technology development project for next generation CO_2 separation, capture and geologic sequestration—production of hydrogen fuel by sorbent enhanced water gas shift reaction, December 01–December 03, Final Report submitted to DOE, 2003.
2. S.G. Mayorga, J.R. Hufton, S. Sircar, T.R. Gaffney, Sorption enhanced reaction process for production of hydrogen, Phase 1 Final Report, U.S. Department of Energy, July 1997.
3. J.R. Hufton, S.J. Weigel, W.F. Waldron, M. Rao, S. Nataraj, S. Sircar, T.R. Gaffney, Final Report: Sorption Enhanced Reaction Process for Production of Hydrogen, DOE-Air Products Cooperative Agreement #DE-FC36-95G010059, 2001.
4. D.J. Borgars, J.S. Campbell, in: A.V. Slack, G. Russel James (Eds.), Carbon Monoxide Conversion II. Design and Operation of CO Shift, Naptha and Natural Gas, Ammonia Part II, 1974, Chapter 4.
5. D.M. Todd, R.A. Battista, Demonstrated applicability of hydrogen fuel for gas turbines, GE power systems, IChemE Gasification 4 Conference, Noordwijk, The Netherlands, 2000.